Random Reflective Surfaces (RRSs) to Enhance MIMO for Terahertz Communications

Suresh Singh
Department of Computer Science
Portland State University
Portland, OR 97207
Email: singh@cs.pdx.edu

Thanh Le
Department of ECE
Portland State University
Portland, OR 97207
Email: thanh4@pdx.edu

Ha Tran
Department of ECE
Portland State University
Portland, OR 97207
Email: tranha@pdx.edu

GLOBECOM 2024 - 2024 IEEE Global Communications Conference | 979-8-3503-5125-5/24/$31.00 ©2024 IEEE | DOI: 10.1109/GLOBECOM52923.2024.10901522

***Abstract*—Line of Sight (LoS) Multiple Input Multiple Output (MIMO) terahertz communication channels suffer from a decrease in capacity in the far field due to the channel matrix only having single rank. Prior work in millimeter wave (mmWave) systems has considered the design of Intelligent Reflective Surfaces (IRSs) to mitigate this problem by introducing phase variation in reflected signals. Given the high cost of IRSs, we propose inexpensive Random Reflective Surfaces (RRSs) to create a rich multi-path environment for terahertz.**

In this work, we build three RRSs using high-density polyethylene (HDPE) sheets embedded with tiny copper flakes at different densities. The reflection behavior of these systems is studied in a terahertz testbed where we focus on the frequency band centered at 410GHz. Using 2x2 MIMO measurements in this testbed, we show that our RRS designs indeed do improve capacity as compared to reflections from polished aluminium (which behaves like a LoS channel). In addition, we examine the range of reflected phase produced and show that, indeed, the high variation in phase leads to improved channel capacity for the case when the channel state information is only available at the receiver (CSIR) for 2x2 MIMO.

***Index Terms*—Terahertz, reflective surfaces, mimo**

I. Introduction

Given severe attenuation suffered by terahertz signals that are naturally reflected in the environment, LoS MIMO is considered the primary mechanism for providing high data rate links at these frequencies. Unfortunately, LoS MIMO capacity is relatively lower in the far field because the channel matrix is single rank [13]. Indeed, the optimal antenna configuration in this case is a directional beam. Millimeter wave systems suffer from a similar problem. In this domain, Intelligent Reflective Surfaces (IRSs) have been studied for enhancing MIMO capacity. In a typical design, using end-to-end channel state information, a centralized controller adjusts the phase of the reflected wave for each antenna element. The controller determines these phase shifts by solving a complex optimization problem for the given communication scenario. It has been shown that this method ensures capacity maximization for MIMO links. Unfortunately, this approach has significant complexity (as we describe in section II) which has hampered deployment of such systems.

This work was funded by the NSF under grants CNS-1910655 and CNS-2416077.

Our work considers the problem of creating a *phase-rich* environment for terahertz channels. Unlike millimeter waves or lower frequencies, terahertz signals are easily blocked, suffer huge attenuation upon reflection from many common surfaces, and are absorbed in the atmosphere. As a result, we cannot rely on the propagation environment to provide a diversity of reflected paths. We propose utilizing reflectors, where each element introduces a random phase into the reflected signal. Unlike IRSs, our design (called RRS) has no controller and doesn't require end-to-end channel knowledge to adjust the reflected phase. Our hypothesis is that such random reflective surfaces will provide a sufficient variation in reflected phase to enable good MIMO channels. Of course, the RRS enabled channels will not be optimal but we believe that their simplicity will enable wide-spread deployment and use.

In this work, we design simple RRSs and characterize their behavior using a terahertz testbed. The RRSs consist of three layers – a large number of randomly placed copper chips on a HDPE plate with an aluminium backing. We present results for 410GHz showing that our reflectors do indeed create a phase-rich set of reflections which enhance channel capacity. We also examine the design of the reflectors by varying the density of reflective elements to determine the relationship between phase distribution and density of the reflectors. We conclude that our designs are excellent at providing a good communication channel for terahertz MIMO.

The remainder of the paper is organized as follows. In the next section we present related work. Subsequently, in section III we discuss the theoretical motivation behind RRSs. Section IV describes the design of our reflective surfaces and we present measurement results in section V. We conclude in section VI.

II. Related Work

Intelligent Reflective Surfaces (IRSs) or Re-configurable Intelligent Surfaces (RISs) have been proposed as a way to improve coverage and enhance capacity of mmWave networks. The typical architecture of these systems consists of m antenna elements placed on a flat surface with the necessary electronics to allow each of the antennas to add a phase shift to the sum

of the incident signals prior to reflecting them [23]. The optimization problem consists of jointly determining the reflected phase (from each element of the IRS) and the transmission power matrix. A centralized controller is assumed to perform these computations given complete channel state information, [8], [23]. In [6] the optimization problem is formulated for the multi-user case in mmWave systems.

Some authors [4], [5] have studied IRSs for terahertz where they add the attenuation behavior of terahertz (i.e., molecular absorption) to the channel model. However, the analysis is based on simulation and modeling, not measurements. IRSs have been considered in other contexts as well. For example, in [21], the authors utilize IRS to enhance self-interference cancellation for in-band full-duplex communication systems. Several authors have explored the use of IRSs in vehicular and aerial networks. [27] provides a survey of using IRSs for 6G vehicular systems. The essential idea is identical to indoor deployments – IRSs are deployed on building facades to improve mmWave coverage.

Some variants of the IRS concept include *programmable/reconfigurable meta-surfaces* [25], [26] where artificial surfaces are designed to allow manipulation of the incident waves in space and frequency domains, *software-defined surfaces* [3] where the IRS is capable of modulation, *passive intelligent reflectors* [12], [16] where a mirror is composed of many small mirrors, each of which can be individually controlled, and *fully passive reflectors*.

Fully passive reflectors have been explored in the context of improving coverage in 5G mmWave cells for urban scenarios. For instance, [18] develops a simple NLoS channel model for reflections from building tops to users on the ground. [1] proposes an optimization framework for the joint placement of gNBs and reflectors in urban geometries in order to improve coverage. [7] considers the reflector placement problem in indoor scenarios where the LoS path of a mmWave AP is obstructed. For indoor terahertz cells, [2] proposes using *reconfigurable* dielectric mirrors placed on all the walls to provide coverage in rooms.

[11], [14] study a NIRS (Non Intelligent RS) for enabling NLoS terahertz links. They build simple reflectors using tinfoil wrapped on foam board and show significant gains in measurement studies at 300-371 GHz. We note that in [22] we measured and modeled the terahertz reflected channel from metal plates as well as from wood and show that these surfaces work well to provide connectivity in NLoS environments. In addition, in [20] we built a *diffusive surface* to also enhance capacity and provided measurements. This latter work is somewhat similar to [11] but our surface produces a lot more reflections.

While there has been a great deal of published work on IRSs (a search of IEEE Conferences yielded over 400 recently published papers), we have not seen any significant commercial deployments. The reason is the complexity of the design which requires solving optimization problems for each user and user location. Unlike IRSs, our approach of using random reflectors is inexpensive and has no operational costs. Of course, the capacity delivered is sub-optimal but we believe that for terahertz, where there is a great deal of available bandwidth, this is a reasonable trade-off. Furthermore, given the blockage problem of terahertz, RRSs provide an attractive alternative to plain reflectors since they additionally boost capacity over LoS.

Finally, there has been a great deal of measurement-based work on terahertz reflections from different surfaces. For instance, there has been work done on terahertz reflections from vehicles [9], indoor materials including drywall, clear glass as well as stratified building materials [15], [24], and different metals [15].

In this paper, we present a novel design of reflective surfaces where, by embedding tiny copper flakes on a neutral medium, we can produce random phase shifts in the reflected signals. We construct three prototypes and perform an exhaustive study of the reflected signal properties. We show that our design does improve capacity because the RRS produces a diversity of phase shifts.

III. Theoretical Background

Let us assume that the transmitter and receiver have N_t and N_r antenna elements respectively. Let d_{ij} be the distance between antenna i of the transmitter and antenna j of the receiver and let d_0 be the distance between the two arrays. Then, the channel response matrix for the LoS channel (assuming omni-directional antennas) can be written as [17], [19],

$$\mathbf{H}_{\text{LoS}} = \frac{\lambda}{4\pi d_0} e^{-\frac{1}{2}\alpha \text{molec}^{(f,T_K,p)d_0}} \left[e^{-jkd_{ij}}\right]_{N_r \times N_t} \quad (1)$$

where, $k = 2\pi/\lambda$ is the wavenumber, f is the frequency, T_K is the temperature in degrees Kelvin, p is the barometric pressure, and α_{molec} is the total molecular absorption at the given frequency. The channel matrix from equation (1) is rank one and has one singular value in the far field [13]. However, if we were to introduce a reflector, then the channel matrix would become,

$$\mathbf{H} = \mathbf{H}_{\text{LoS}} + \mathbf{H}_{\text{R}} \quad (2)$$

where the second term corresponds to the reflected channel.

Let us assume that the reflective surface consists of M elements *and each element m adds a phase of ϕ_m to the reflected signal*. Then, we have $M \times N_t \times N_r$ total reflected paths between the transmitter and the receiver. We can write the channel matrix as,

$$\mathbf{H}_{\text{R}} = \sum_{m=1}^{M} \alpha_m e^{j\phi_m} \left[e^{-jkd_{im}} e^{-jkd_{mj}}\right]_{N_r \times N_t} \quad (3)$$

where $\alpha_m \in \mathbb{C}$ is the channel gain for the mth reflective element, d_{im} is the distance from the ith transmit antenna to the mth reflective element and d_{mj} is the distance from the mth reflective element to the j receiver antenna. The channel gain for the reflective elements can be written as $\alpha_m = ae^{-j\psi_m}$ where $\psi_m = k(d_{tm} + d_{rm})$ and d_{tm}, d_{rm} are the distance of the transmitter and receiver from the mth element respectively. The value of $a \in \mathbb{R}$ (the attenuation

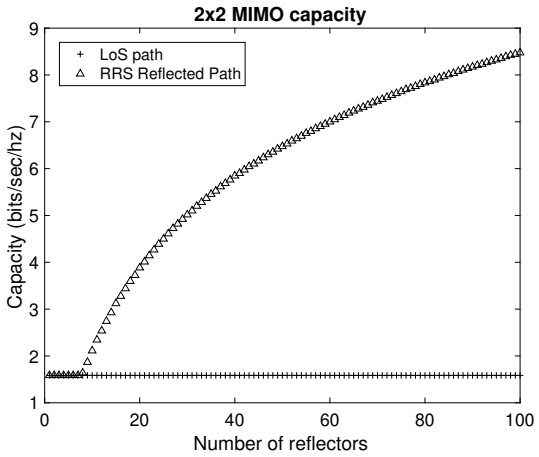

Fig. 1. Capacity improvement with fixed random phase.

constant) depends on the radiation pattern of the reflective element. For instance, for a square reflective element with side equal to $\lambda/2$,

$$a = \frac{\lambda^2}{14\pi d_{tm} d_{rm}} (cos(\beta_{tm}) cos(\beta_{rm})^q \tag{4}$$

where β_{tm} and β_{rm} are the angles between the normal to the m element and the vector connecting it to the transmitter and receiver, respectively. For the square shape with the given dimensions, $q \sim 0.285$ [10]. Of course, different shaped elements will have a different a. By combining equations (3) and (4), we obtain the complete channel model for the reflected channel.

The capacity of the channel can be written as,

$$\mathcal{C} = \log_2 \det \left[\mathbf{I}_{N_r} + \frac{1}{\sigma^2} \mathbf{H} \mathbf{Q} \mathbf{H}^\dagger \right] \tag{5}$$

where σ^2 is the noise variance, $\mathbf{Q} \in \mathbb{C}^{N_t \times N_t}$ is the covariance matrix of the transmitted signal with $tr(\mathbf{Q}) \leq P$, where P is the total transmitted power.

The typical problem addressed in the IRS literature is the joint optimization of the power budget of each transmit antenna $\mathbf{Q}$ and the phase ϕ_m that is applied to each element of the IRS.

A. Simplification for the RRS Case

We can simplify the above formalism to the case when we use RRSs. Since we are considering a CSIR channel, the transmit power allocated to each transmit antenna is the same and hence the $\mathbf{Q}$ matrix reduces to the identity matrix multiplied by P/N_t in equation 5. Let us denote by $\boldsymbol{\phi} = \{\phi_1, \phi_2, \cdots, \phi_M\}$ the *fixed* phases of each of the reflective elements of the RRS, equation 3. We evaluated equation 5 using randomly assigned phases for a 2x2 MIMO system where the distance between the transmitter and receiver is 10m and the distance of the reflector to the line connecting the transmitter and receiver is 5m. The antenna spacing is assumed to be $\lambda/2 = 1$mm corresponding to a frequency of 300GHz. Figure 1 plots the capacity as a function of the number of elements M in the RRS. The capacity is an average of 100 runs where elements are assigned uniform random phases in the range $[0, \pi/2]$ for each run. Observe that for the LoS case, the capacity is 1.585 bits/sec/hz (note that the distance is fixed in this plot). However, if we use the reflected path, the capacity begins to increase for $M > 40$ elements. This is similar to the observation in [28] where IRS with greater than 50 elements is shown to deliver higher capacity than LoS.

IV. Design of our RRSs

In this paper, we aim to create a multi-path environment using random distribution of copper chips on a HDPE sheet, which we call Random Reflective Surfaces (RRSs). Figure 2 illustrates step-by-step procedure to fabricate a RRS prototype. Starting with a 6"x6" HDPE sheet of 1/4" thickness, we melt one side of HDPE sheet at 350^{o}C for 5 minutes. Once a visible melting layer is observed, we randomly sprinkle the copper chips onto the HDPE sheet. The copper chips have a mean size of 0.4 mm. After that, we leave the HDPE sheet to cool down again with the copper chips attached to its surface and thus we have our RRS. To explore how the effect of copper chip density, we fabricate three different RRSs using the same procedure above. Figure 3 shows the top surface of three RRSs with different level of copper chips density.

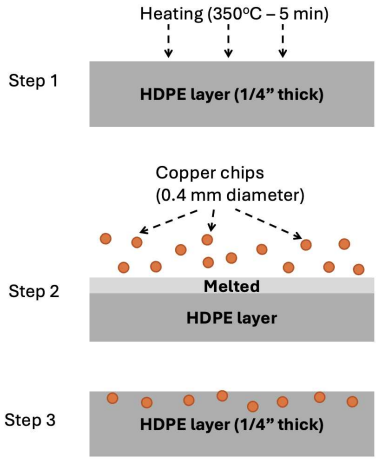

Fig. 2. Step by step procedure of RRS fabrication

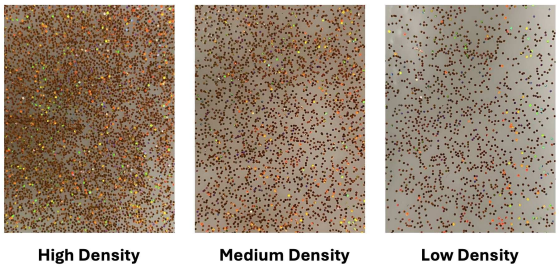

Fig. 3. Top surface of designed RRSs showing three level of copper chip density

The ideal phase shift caused by the copper chips can be written as $2\pi L/\lambda$ where L is the length of the copper chip. Thus, the average phase shift at 410 GHz signal will have is approximately 197^o. However, many copper chips touch each other which increases the effective length L. Similarly, some fractions of chips are shorter than 0.4mm and those will result in smaller phase shift. It is also noteworthy that surface of the reflector is not smooth – the copper chips are embedded to slightly differing depths randomly. Taking all these factors into consideration, we end up with a random reflector.

V. Measurements and Results

We employ a Vector Network Analyzer (VNA) from Rohde & Schwartz and frequency extender modules from Virginia Diode, Inc. (VDI) to collect elements of the transfer matrix H_{ij}. In this paper, the WR2.2 band extender module, generating signals from 325 GHz to 500 GHz, is used for measurements at the frequency of 410 GHz. The system is calibrated using Thru-Reflect-Line (TRL) standards to eliminate mismatched effects from cables and connections prior to conducting measurements. With TRL calibration, the waveguide openings of TX and RX become the measurement reference plane. Other VNA settings include the output power of 5 dBm, IF bandwidth of 1 kHz, and an averaging factor of 10. The setup uses a pair of 1.68 cm long antennas with 25dB gain to transmit and receive signals. The 2x2 MIMO measurement is performed where signals are reflected by our RRSs or an aluminium plate. Figure 4 demonstrates the measurement setup for the medium-density RRS. The angle of incidence is 45^o and the inter-antenna spacing is 0.89 cm for aluminium plate and all RRSs setups. We vary the transmitter-receiver (TX-RX) distance (measured from TX's antenna aperture to RX's) from 37 cm to 49 cm with a 3.175 mm increment. *We note that all measurements are only for the reflected channel – there are no LoS components.* This is done to clearly analyze the quality of the reflections produced by the RRS.

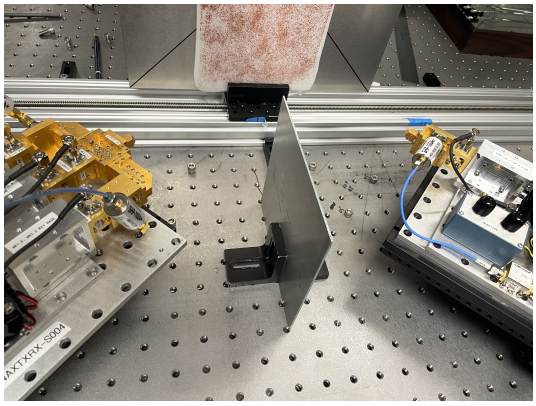

Fig. 4. Front view of the measurement setup for RRS with medium copper chip density

Using the empirical channel matrix and using the fact that this is a CSIR channel, we can easily compute the channel capacity using equation 5. Figure 5 plots the normalized capacity as a function of distance for the three RRS surfaces and for the case when we use a smooth aluminium plate. The aluminium plate acts as an almost perfect reflector and thus behaves like a LoS channel [22] thus providing a point of comparison with the RRSs we propose. We observe that two of our reflectors consistently provide higher capacity than the aluminium plate. Indeed, the medium density RRS has the best performance overall. This supports our claim in this paper that we can create a rich MIMO channel using simple reflectors, rather than IRSs.

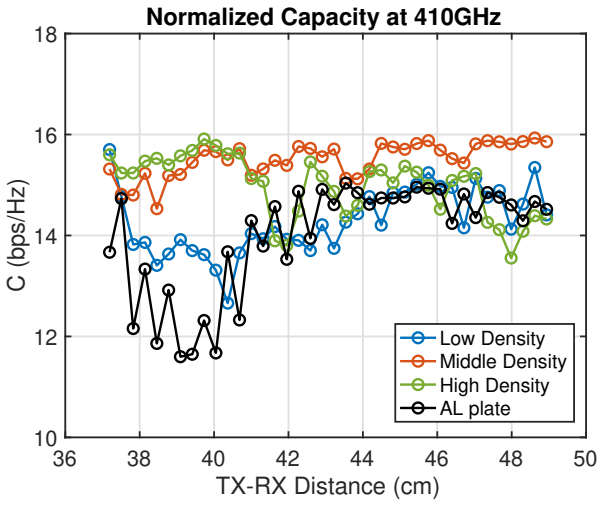

Fig. 5. Normalized capacity over various TX-RX distances

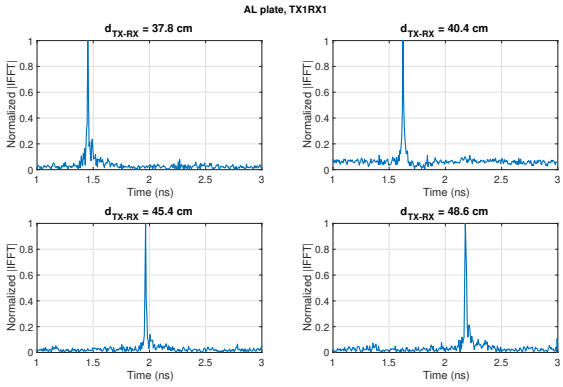

Fig. 6. Normalized IFFT for some distances of signal reflected from AL plate

A. Analysis of Phase Diversity

In order to better explain the capacity plot, we dig deeper into the channel data to identify the range of phases present in the reflected signal. First, we plot the IFFT (Inverse Fast Fourier Transform) for the aluminium plate and the medium density RRS in Figures 6 and 7. We immediately see that the aluminium plate only produces one reflection whereas we see several reflections for the medium density RRS. The same phenomenon with multiple reflections is also observed for high

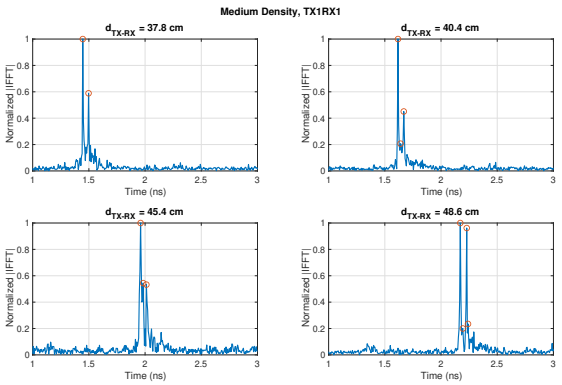

Fig. 7. Normalized IFFT for some distances of signal reflected from RRS with medium copper chip density

density and low density RRS designs. We point out that even though the number of copper chips is quite large, we only get a few distinct phases because most of the copper chips are the same length and hence there is no phase variation in their reflections.

We utilize the IFFT plots for each distance and each RRS to identify the significant reflected components. For a given IFFT, we consider all reflections that have at least 0.2x the magnitude of the largest component, see Figure 8. Next, we determine the time of arrival of each of these components relative to the first component. Then we set the phase of the main component to zero and compute the phase offset of each of these reflections using the frequency of 410GHz.

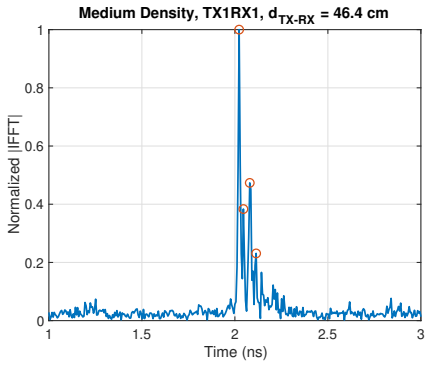

Fig. 8. Identifying the significant reflected components.

In Figures 9, 10, and 11 we plot the histogram for each of the three RRS designs (we combine the data for all 38 distances for this). The phase variance for the three designs is shown in Table I.

Interestingly, we note that the average phase variance is highest for the medium density RRS, which also shows the highest capacity across distances. The aluminium plate has a single reflection and therefore we do not plot its histogram. Finally, consider Figure 1 where we plot the capacity versus number of reflectors.

TABLE I
VARIANCE IN PHASE FOR RRSS WITH DIFFERENT COPPER CHIPS DENSITY

Copper Chips Density	Variance in phase
Low	1.00e+04
Medium	1.12e+04
High	1.02e+04

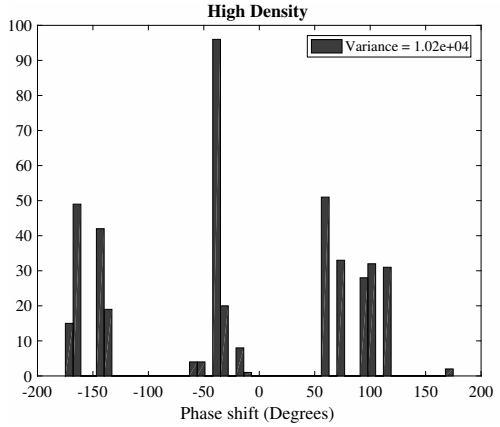

Fig. 9. Histogram of reflected phase for high-density RRS.

VI. CONCLUSIONS

We consider the problem of artificially creating a rich multi-path environment for terahertz communications by using random reflective surfaces (RRSs). Unlike IRSs, where a controller optimizes the reflected phase of each reflecting element, we utilize a collection of random reflectors which introduce a random phase into their reflections. We constructed three such reflectors using HDPE embedded with copper flakes and empirically verified that our design does improve 2x2 MIMO capacity. We conducted a further examination of the reflected phase and documented the range of phase produced by each RRS. We show that the RRS design with the highest capacity is also the one that has the most phase variation among the designs.

Our future work involves construction of more diverse reflectors utilizing the theory described here. We will additionally extend our work to mmWave systems as those systems are currently being deployed and can benefit from a RRS like design.

REFERENCES

[1] Chethan Kumar Anjinappa, Fatih Erden, and Ismail Güvenç. Base station and passive reflectors placement for urban mmwave networks. *IEEE Transactions on Vehicular Technology*, 70(4):3525–3539, 2021.

[2] Michael Taynnan Barros, Robert Mullins, and Sasitharan Balasubramaniam. Integrated terahertz communication with reflectors for 5g small-cell networks. *IEEE Transactions on Vehicular Technology*, 66(7):5647–5657, 2017.

[3] Ertugrul Basar. Reconfigurable intelligent surface-based index modulation: A new beyond mimo paradigm for 6g. *IEEE Transactions on Communications*, 68(5):3187–3196, 2020.

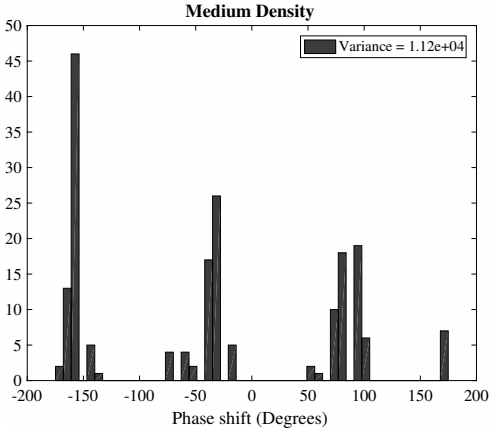

Fig. 10. Histogram of reflected phase for medium density RRS.

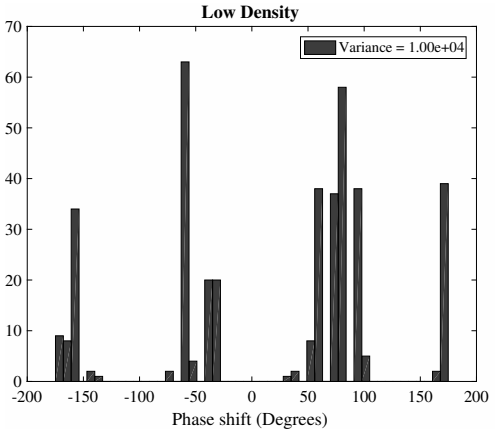

Fig. 11. Histogram of reflected phase for low density RRS.

[4] Alexandros-Apostolos A. Boulogeorgos and Angeliki Alexiou. Coverage Analysis of Reconfigurable Intelligent Surface Assisted THz Wireless Systems. *IEEE Open Journal of Vehicular Technology*, 2:94–110, 2021.

[5] Alexandros-Apostolos A. Boulogeorgos, Nestor Chatzidiamantis, Harilaos G. Sandalidis, Angeliki Alexiou, and Marco Di Renzo. Performance Analysis of Multi-Reconfigurable Intelligent Surface-Empowered THz Wireless Systems. In *Proceedings of IEEE ICC*, Feb 2022.

[6] Yashuai Cao, Tiejun Lv, and Wei Ni. Intelligent reflecting surface aided multi-user mmwave communications for coverage enhancement. In *2020 IEEE 31st Annual International Symposium on Personal, Indoor and Mobile Radio Communications*, pages 1–6, 2020.

[7] Ang Deng, Yuchen Liu, and Douglas M. Blough. Maximizing coverage for mmwave wlans with dedicated reflectors. In *ICC 2021 - IEEE International Conference on Communications*, pages 1–6, 2021.

[8] Hongyang Du, Jiayi Zhang, Ke Guan, Dusit Niyato, Huiying Jiao, Zhiqin Wang, and Thomas Kürner. Performance and Optimization of Reconfigurable Intelligent Surface Aided THz Communications. *IEEE Transactions on Communications*, 70(5):3575–3593, May 2022.

[9] Johannes M. Eckhardt, Vitaly Petrov, Dmitri Moltchanov, Yevgeni Koucheryavy, and Thomas Kürner. Channel Measurements and Modeling for Low-Terahertz Band Vehicular Communications. *IEEE Journal on Selected Areas in Communications*, 39(6):1590–1603, June 2021.

[10] S. W. Ellingson. Path loss in reconfigurable intelligent surface-enabled channels. In *2021 IEEE 32nd Annual International Symposium on Personal, Indoor and Mobile Radio Communications (PIMRC)*, pages 829–835, 2021.

[11] Chong Han, Yuanbo Li, Yiqin Wang, and Ziming Yu. Still waters run deep: Extend thz coverage with non-intelligent reflecting surface. *Wireless Commun.*, 31(1):41–47, feb 2024.

[12] Chongwen Huang, Alessio Zappone, Mérouane Debbah, and Chau Yuen. Achievable rate maximization by passive intelligent mirrors. In *2018 IEEE International Conference on Acoustics, Speech and Signal Processing (ICASSP)*, pages 3714–3718, 2018.

[13] Emad Ibrahim, Rickard Nilsson, and Jaap van de Beek. Intelligent reflecting surfaces for mimo communications in los environments. In *2021 IEEE Wireless Communications and Networking Conference (WCNC)*, pages 1–6, 2021.

[14] Yuanbo Li, Yiqin Wang, Yi Chen, Ziming Yu, and Chong Han. Channel measurement and coverage analysis for nirs-aided thz communications in indoor environments. *IEEE Communications Letters*, 27(9):2486–2490, 2023.

[15] Jianjun Ma, Rabi Shrestha, Lothar Moeller, and Daniel M. Mittleman. Invited Article: Channel performance for indoor and outdoor terahertz wireless links. *APL Photonics*, 3(5):051601, May 2018.

[16] Deepak Mishra and Håkan Johansson. Channel estimation and low-complexity beamforming design for passive intelligent surface assisted miso wireless energy transfer. In *ICASSP 2019 - 2019 IEEE International Conference on Acoustics, Speech and Signal Processing (ICASSP)*, pages 4659–4663, 2019.

[17] Anamaria Moldovan, Michael A. Ruder, Ian F. Akyildiz, and Wolfgang H. Gerstacker. Los and nlos channel modeling for terahertz wireless communication with scattered rays. In *2014 IEEE Globecom Workshops (GC Wkshps)*, pages 388–392, 2014.

[18] Zhangyou Peng, Linxiao Li, Miao Wang, Zhonghao Zhang, Qi Liu, Yang Liu, and Ruoran Liu. An effective coverage scheme with passive-reflectors for urban millimeter-wave communication. *IEEE Antennas and Wireless Propagation Letters*, 15:398–401, 2016.

[19] I. Sarris and A. R. Nix. Maximum mimo capacity in line-of-sight. In *International Conference on Information Communications and Signal Processing*, Bankok, Thailand, 6-9 December 2005.

[20] S. Singh, H. Tran, and T. Le. Stabilizing terahertz mimo channel capacity with controlled diffuse reflections. In *2023 IEEE International Conference on Communications*, May 2023.

[21] Simon Tewes, Markus Heinrichs, Paul Staat, Rainer Kronberger, and Aydin Sezgin. Full-Duplex meets Reconfigurable Surfaces: RIS-assisted SIC for Full-Duplex Radios. In *ICC 2022 - IEEE International Conference on Communications*, pages 1106–1111, May 2022.

[22] Ha Tran, Thanh Le, and Suresh Singh. Reflection Channel Model for Terahertz Communications. In *2022 IEEE International Conference on Communications*, June 2022.

[23] Peilan Wang, Jun Fang, Xiaojun Yuan, Zhi Chen, and Hongbin Li. Intelligent reflecting surface-assisted millimeter wave communications: Joint active and passive precoding design. *IEEE Transactions on Vehicular Technology*, 69(12):14960–14973, 2020.

[24] Yunchou Xing, Ojas Kanhere, Shihao Ju, and Theodore S. Rappaport. Indoor Wireless Channel Properties at Millimeter Wave and Sub-Terahertz Frequencies. In *2019 IEEE Global Communications Conference (GLOBECOM)*, pages 1–6, December 2019.

[25] L. Zhang, X. Q. Chen, S. Liu, Q. Zhang, J. Zhao, J. Y. Dai, G. D. Bai, X. Wan, Q. Cheng, G. Castaldi, V. Galdi, and T. J. Cui. Space-time-coding digital metasurfaces. In *2019 Thirteenth International Congress on Artificial Materials for Novel Wave Phenomena (Metamaterials)*, pages X–128–X–130, 2019.

[26] Jie Zhao, Xi Yang, Jun Yan Dai, Qiang Cheng, Xiang Li, Ning Hua Qi, Jun Chen Ke, Guo Dong Bai, Shuo Liu, Shi Jin, Andrea Alù, and Tie Jun Cui. Programmable time-domain digital-coding metasurface for non-linear harmonic manipulation and new wireless communication systems. *National Science Review*, 6(2):231–238, 11 2018.

[27] Yishi Zhu, Bomin Mao, and Nei Kato. Intelligent reflecting surface in 6g vehicular communications: A survey. *IEEE Open Journal of Vehicular Technology*, 3:266–277, 2022.

[28] Özgecan Özdogan, Emil Björnson, and Erik G. Larsson. Using intelligent reflecting surfaces for rank improvement in mimo communications. In *ICASSP 2020 - 2020 IEEE International Conference on Acoustics, Speech and Signal Processing (ICASSP)*, pages 9160–9164, 2020.